J Solid State Electrochem (2012) 16:253–263
DOI 10.1007/s10008-011-1314-y

ORIGINAL PAPER

Efficient maximization of coloration by modification in morphology of electrodeposited NiO thin films prepared with different surfactants

Dhanaji S. Dalavi · Meenatai J. Suryavanshi · Sawanta S. Mali · Dipali S. Patil · Pramod S. Patil

Received: 17 July 2010 / Revised: 17 November 2010 / Accepted: 14 January 2011 / Published online: 8 February 2011

Abstract In this paper, we report on the nickel oxide (NiO) thin films potentiostatically electrodeposited onto indium-doped tin oxide-coated glass substrates by using two types of organic surfactants: (1) non-ionic: polyethylene glycol (PEG), polyvinylpyrrolidone (PVP) and (2) anionic: sodium dodecyl sulfate (SDS). An aqueous solution containing nickel sulfate precursor and potassium hydroxide buffer was used to grow the samples. The effect of organic surfactants on its structural, morphological, wettability, optical, electrochromic, and in situ colorimetry were studied using X-ray diffraction, scanning electron microscopy, contact angle, FT-IR spectroscopy, optical transmittance, cyclic voltammetry, and CIE system of colorimetry. X-ray diffraction patterns show that the films are polycrystalline, consisting of NiO cubic phase. A nanoporous structure with pore diameter of about 150–200 nm was observed for pure NiO. The films deposited with the aid of organic surfactants exhibits various surface morphological feature. PVP-mediated NiO thin film shows noodle-like morphology with well-defined surface area whereas, an ordered pore structure composed of channels of uniform diameter of about 60–80 nm was observed for PEG. A compact and smooth surface with nanoporous structure stem from SDS helps for improved electrochromic performance compared with that of NiO deposits from surfactant-free solution. Wetting behavior shows, transformation from hydrophilic to superhydrophilic nature of NiO thin films deposited with organic surfactant, which helps for much more paths for electrolyte access. The surfactant-mediated NiO produce high color/bleach transmittance difference up to 57% at 630 nm. On oxidation of NiO/SDS, the CIELAB 1931 2° color space coordinates show the transition from colorless to the deep brown state (L^*=84.41, a^*=−0.33, b^*=4.41, and L^*=43.78, a^*=7.15, b^*=13.69), with steady decrease in relative luminance. The highest coloration efficiency of 54 cm^2 C^{-1} with an excellent reversibility of 97% was observed for NiO/SDS thin films.

Keywords NiO thin films · Organic surfactants · Morphology · Contact angle · Electrochromic properties · Colorimetric analysis

Introduction

Electrochromism is the process by which a material can exhibit a reversible and persistent color change upon insertion/extraction of Li^+ or OH^- ions with applied potential [1]. In recent years, nickel oxide (NiO) thin films have received a great interest due to its applications in diverse fields, such as large-scale optical switching glazing, electronic information display [2], gas sensors [3], tandem dye-sensitized solar cells [4], magnetic materials [5], transparent organic light emitting diode [6], and catalysis [7].

Surface modification is an important area of study in modern electrochemistry, and any research carried out in this direction will be of interest, especially due to the several application possibilities of these electrodes [8]. Recently, nanostructured materials with various surface morphologies attracted great deal of attention in nanotech-

Electronic supplementary material The online version of this article (doi:10.1007/s10008-011-1314-y) contains supplementary material, which is available to authorized users.

D. S. Dalavi · M. J. Suryavanshi · S. S. Mali · D. S. Patil · P. S. Patil (✉)
Thin Films Materials Laboratory, Department of Physics, Shivaji University,
Kolhapur 416004, MS, India
e-mail: psp_phy@unishivaji.ac.in

nology for an intended application [9–13]. The synthesis of varieties of surface morphologies form ordered superstructures or complex functional architectures offer great opportunities to explore their novel properties for fabrication of various nano-devices, research, and development across the globe concentrating on invention of various nanostructures [14, 15]. The amphiphilic nature of organic surfactants helps in modifying the surface morphology of the deposit owing to their concentration-dependent specific activity during electrodeposition [16]. The specific activity of the surfactants is generally understood in terms of adsorption at the cathode surface during deposition and depends on the critical micelle concentration of the surfactant molecules which forms the bilayer or multilayer at the electrode interface [17]. Effect of organic surfactants on metals such as Tl(I), Pb(II), Cd(II), Cu (I1), and In(II1) [18], as well as oxide including ZnO [16], WO_3 [19], and NiO [20–22] have been investigated extensively during past decade.

Plethora of chemical and physical techniques have been used to deposit NiO thin films, such as chemical bath deposition [23], sol–gel technique [24], spray pyrolysis [25], hydrothermal synthesis [26], electrodeposition [27], chemical vapor deposition [28], pulse laser deposition [29], electron beam evaporation technique [30], RF magnetron sputtering [31], and DC magnetron sputtering [32]. Among all methods mentioned above, electrodeposition of NiO thin films for EC devices has been sparse, although this technique allows tailoring the properties of NiO thin films by adjusting the deposition parameters.

In this paper, we have systematically demonstrated the effect of organic surfactants, such as anionic and non-ionic surfactants on the electrochemical deposition of NiO and the resulting changes on the structural, morphological, wettability, and colorimetric analysis of the electrodeposits. Anionic and non-ionic surfactants have been used to investigate the effect of the charge of head groups on the electrodeposition process. Our investigation from colorimetric analysis shows that the NiO thin films incorporating the organic surfactants exhibits better kinetics of coloration and bleaching in comparison to pure NiO thin films electrodeposits. However, there are only few investigations on the colorimetric analysis of inorganic metal oxides. The main object of this paper is to elucidate the effect of organic surfactant on the microstructure properties NiO thin films and on coloration and bleaching kinetics of electrodeposits.

Experimental

Synthesis

NiO thin films have been synthesized using two different electrochemical routes: (1) without organic surfactant and (2) with organic surfactants. In the first route, 0.5 M $NiSO_4{\cdot}6H_2O$ (Loba Chemie, 99%) aqueous solution and 1 M KOH was used as buffer in order to increase the pH of the final solution. The thin films of NiO were obtained by potentiostatic electrodeposition at 1V (vs SCE) in an aqueous solution with pH of 7.4 and deposited for 30 min in a three-electrode electrochemical cell comprising an indium-doped tin oxide (ITO; Kintec corp. Ltd, Hong Kong) coated conducting glass substrate with a sheet resistance of 20–25 Ω cm^{-2} were used as working electrode, a platinum wire as a counter electrode, and a saturated calomel electrode (SCE) as a reference electrode.

Furthermore, to study the effect of organic surfactants on the growth of NiO deposits and their properties, various organic surfactants, such as polyvinylpyrrolidone (PVP, 130,000 g mol^{-1}, Alfa Aesar), polyethylene glycol (PEG, 20,000 g mol^{-1}, Himedia), and sodium dodecyl sulfate (SDS, 288.33 g mol^{-1}, Sd fine, 99.5%) were added separately in a definite proportion. The concentration of organic surfactants (polymers) was kept constant at 0.5 wt. % in the final solution. All the experiments were performed in quiescent solution at room temperature. Furthermore, these films were annealed at 300 °C in air for 90 min. Prior to deposition, ITOs were cleaned with ultrasonic vibrations in acetone and de-ionized water, respectively. The film prepared by using different organic surfactants, such as PVP, PEG, and SDS abbreviated as NiO/PVP, NiO/PEG, NiO/SDS, and those without organic surfactant are denoted NiO.

Characterizations

The structural properties of the films were studied by X-ray diffraction (Philips, PW 3710, Almelo, Holland, operated at 40 kV, 25 mA with Cr Kα radiation, λ=2.2897 Å). The infrared (IR) spectrum of powder collected from all NiO samples were recorded using Perkin–Elmer IR spectrophotometer (model-100) in the spectral range of 400–4,000 cm^{-1}. The pellets were prepared by mixing KBr with NiO powder collected by scratching film from glass substrates, in the ratio 300:1 and then pressing the powder between two pieces of polished steel. The surface morphology of the films was examined by scanning electron microscopy (SEM; Model JEOL-JSM-6360, Japan, operated at 20 kV) with a thin layer of gold sputter coated prior to analyses. The optical transmittance spectra of fully colored and fully bleached states were measured over the range of 350–1,000 nm using an UV-vis spectrophotometer (Shimadzu, model: UV-1800, Japan). All the electrochromic measurements were performed in an electrolyte (1 M KOH) in a conventional three-electrode arrangement comprising platinum wire as the counter electrode and SCE serving as the reference electrode using electrochem-

ical quartz crystal measurements (model-CHI-400A) made by CH Instruments, USA.

Colorimetric determinations were done with the help of Shimadzu color analysis software by analyzing the transmittance spectra of color/bleach state to evaluate the $L^*a^*b^*$ and Yxy coordinate values. These obtained values were used as reference data in order to get the observed color in reduced and oxidized state for all samples from online color analysis software with 1931 2° observer and D-65 illuminant proposed by CIE Yxy and $L^*a^*b^*$ coordinate.

Results and discussion

Formation of NiO thin films

Potentiostatic deposition in a transition metal bath leads to the formation of oxide or hydroxide depending upon the stability of resultant deposits. In the case of electrodeposition of an aqueous solution of nickel sulfate, the oxidation of Ni^{2+} to Ni^{3+} leads to formation of unstable nickel oxyhydroxide which is then finally deposited in the form of $Ni(OH)_2$ on the electrode surface and annealing at 300 °C in air for 90 min leads to the formation of NiO. The overall reaction mechanism can be schematically represented as [33]. NiO(OH)

$$Ni^{2+} \xrightarrow{-e^-} Ni^{3+} \xrightarrow{OH^-} NiO(OH) \underset{e^-}{\rightleftharpoons} Ni(OH)_2 \quad (1)$$

$$Ni(OH)_2 \xrightarrow{\Delta \approx 300^\circ C} NiO + H_2O \uparrow \quad (2)$$

Upon the addition of anionic surfactants (for example, SDS) into an inorganic electrolyte solution (in this context, designated as $NiSO_4{\cdot}6H_2O$), the electrostatic interaction results in the complexation of Ni^{2+}/SDS, comprised of metal cations and anionic head groups of surfactants [34].

X-ray diffraction

Figure 1a–d shows the X-ray patterns of electrodeposited NiO thin film on ITO-coated conducting glass substrates with and without surfactants, annealed at 300 °C for 90 min in an ambient air. All the films are polycrystalline and can be characterized by a cubic structure of NiO with the predominant peak at 43.27° corresponding to the (200) preferred orientation. The XRD patterns of film made with and without surfactants showed no difference. This suggests that the organic surfactants do not affect the crystallographic orientation of NiO. All the peaks in the patterns are indexed according to JCPDS data card of NiO (78-0643).

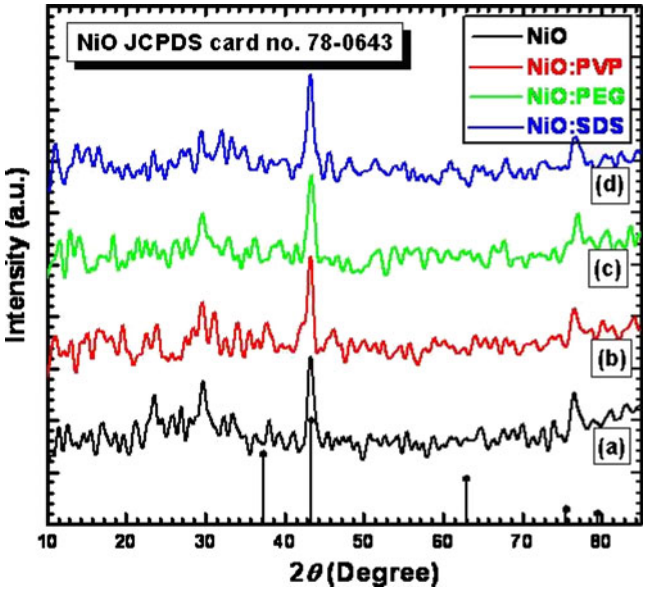

Fig. 1 XRD patterns for **a** NiO, **b** NiO/PVP, **c** NiO/PEG, and **d** NiO/SDS thin films deposited onto ITO-coated conducting glass substrates, annealed at 300 °C for 90 min in ambient air

FT-IR analyses

The IR transmittance spectra of NiO, NiO/PVP, NiO/PEG, and NiO/SDS thin films are shown in Fig. 2a–d. The band at 470 cm^{-1} is due to NiO and assigned to Ni–O interaction [35]. The splitting of the peaks in the spectral region of 988–1,150 cm^{-1} and the shoulder at 636 cm^{-1} belong to free sulfate ions [23, 36]. The vibrations due to carboxyl group are obtained in the range of 1,371–1,463 cm^{-1}. The bands centered at 1,630 and 1,746 cm^{-1} are the characteristics of bending vibration of water and the carbonate ions [37]. The peaks in the spectral region of 2,847–2,923 cm^{-1} for all the samples were attributed to alkyl group [16]. The bands at 3,200–3,600 cm^{-1} correspond to the O–H mode of vibration, i.e., due to the hydroxyl group. These observations indicate that the samples are free from organic surfactants.

Morphological study

Figure 3a shows a SEM image of NiO thin film deposited on ITO-coated glass substrate for 30 min without any surfactant. These reveal that the interconnected nano-flakes network with pore diameter of about 150–200 nm with well-defined cracks. Figure 3b shows a SEM image of PVP-mediated NiO thin film exhibiting noodle-like structure without cracks. Figure 3c shows the SEM image of NiO thin film deposited using PEG. It possesses a well-

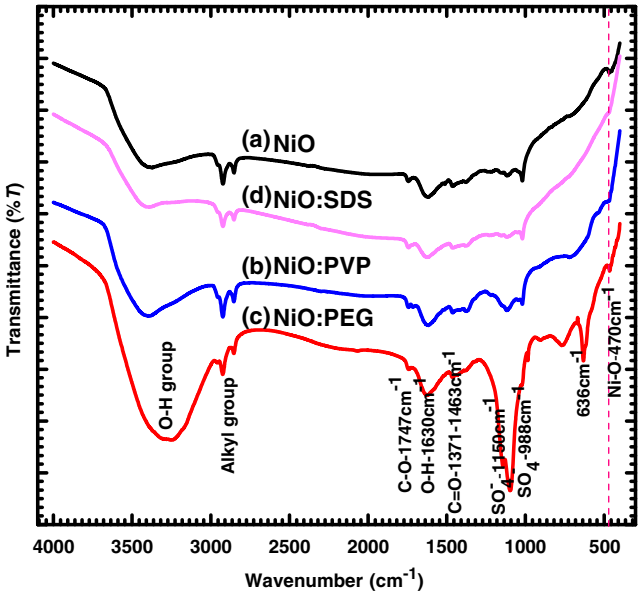

Fig. 2 FT-IR spectra of electrochemically deposited **a** NiO, **b** NiO/PVP, **c** NiO/PEG, and **d** NiO/SDS thin films, annealed at 300 °C for 90 min in ambient air

ordered pore network composed of channels of uniform diameter of about 60–80 nm. Figure 3d shows the SDS-mediated NiO thin film which exhibits a smooth and highly nanoporous network. Interestingly, the films deposited with the aid of surfactant have smaller pores as compared with that of the film deposited without surfactant. This suggests that the electrochemically accessible surface area must be greater than samples grown without surfactant. This high surface area coupled with nanoporosity provides easy path for electrolyte penetration which is helpful for the improvement in EC performance. Figure 4a–d shows the cross-section images of NiO, NiO/PVP, NiO/PEG, and NiO/SDS having thickness of 202, 163, 176, and 229 nm, respectively.

Contact angle measurement

The wettability of solid surfaces with liquids is governed by both their chemical modifications and geometrical structures of the surface. The result of contact angle for NiO thin film with and without surfactants is shown in Fig. 5a–d. As seen from SEM images (Fig. 3a), due to the entrapment of air in hollow porous structure of NiO thin film, liquid air interface has been formed inhibiting electrolyte penetration into film structure and result in contact angle of about 64.28° for pure NiO thin film. However, as anticipated, the introduction of the surfactants (PVP, PEG, SDS) transformed it from hydrophilic to superhydrophilic nature with contact angle of about 12.64°, 11.34°, and 10° that causes large amount of electrolyte access into the film structure and subsequent positive impact on their electrochromic performance. This is due to most commonly encountered amphiphilic surfactants (SDS) consist of a hydrophobic tail group attached to a hydrophilic head group. It is energetically preferential for the surfactant molecules to migrate to the fluid interface or to the substrate where they can play a crucial role in either altering the wettability of the substrate by reducing surface tension of the free surface [37]. Surfactants do affect the wetting property of the electrodeposited NiO samples [38].

Optical absorption

Figure 6a–d shows plots of $(\alpha h\nu)^2$ as a function of the photon energy $(h\nu)$ for NiO thin films deposited onto ITO-coated conducting glass substrates with the aid of various surfactants. The optical absorption data were analyzed using the following classical relation for near edge optical absorption in semiconductor [1]

$$\alpha = \alpha_0 \frac{(h\nu - E_g)^n}{h\nu} \tag{3}$$

where E_g is the optical energy gap between bottom of the conduction band and top of the valence band, $h\nu$ is the photon energy, and n is a constant whose value is ½ for direct transition and 2 for indirect transition. Figure 6a–d implies direct band gap energy of the films from 2.90 to 3.22 eV, which is attributed to the increase in absorbance of films with increase in film thickness of the resultant deposits that causes large number of atoms available for absorption of photon energy and similar band gap narrowing effect has been reported by other authors [20, 39, 40]. The inset of Fig. 6 shows the spectral behavior of absorbance coefficient (α) vs wavelength for NiO, NiO/PVP, NiO/PEG, and NiO/SDS.

Electrochromic properties of NiO thin films

Cyclic voltammetry

The cyclic voltammograms (CVs) of the NiO thin films were recorded at a scan rate of 50 mV s^{-1} in 1 M KOH electrolyte with linear potential sweep between 1.4 to −1 V versus SCE after five cycles (in Fig. 7a–d). The cathodic and anodic peaks observed at −0.5 V and +0.76 are attributed to the redox reaction involving Ni^{2+}/Ni^{3+} transformation. The coloration and bleaching of the film is associated with the deintercalation and intercalation of OH^- ions or extraction of $H^{\pm}$ ions and the redox equation. A simplified reduction scheme implying the gradual change in the optical density upon intercalation/deintercalation of ions in electrochromic NiO film is represented by following equations [41].

$$NiO + xOH \rightleftharpoons NiOOH + xe^- \text{----------} \tag{4}$$

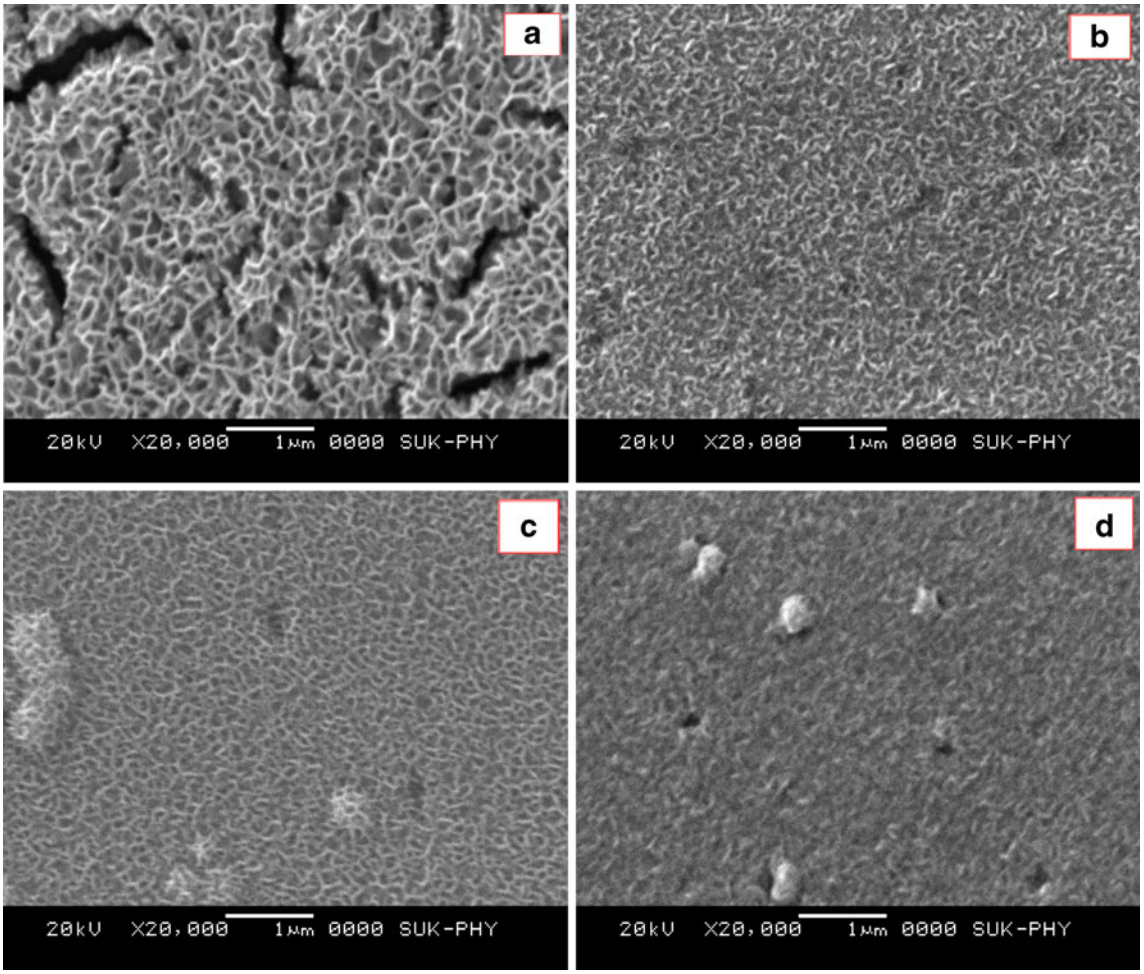

Fig. 3 Typical SEM images of **a** NiO, **b** NiO/PVP, **c** NiO/PEG, and **d** NiO/SDS thin films

During the cathodic scan, the reduction of Ni^{3+} to Ni^{2+} leads to bleaching of the film (cathodic peak at −0.5 V). In the reverse anodic scan, the oxidation of Ni^{2+} to Ni^{3+} causes the coloration of the film (anodic peak at 0.76 V). The corresponding digital photographs at different potentials have been shown in Fig. 8a–d. The general features of the CVs with and without surfactants are similar except the magnitude of the anodic and cathodic peak current density which is similar to the NiO deposited by sol–gel and potentiostatic electrodeposition techniques [27, 42]. The anodic and cathodic peak current density of NiO/SDS thin film are 3.65 and 4.2 mA cm^{-2}, respectively. These values are higher than those obtained for NiO, NiO/PEG, and NiO/PVP. This is mainly due to the electrochemically accessible high surface area of NiO/SDS providing much more path for electrolyte penetration, as supported by contact angle measurements. Injection of ions into the NiO film, two circumstances should be considered, one being the movement of ions in the film and the other being the crossover of ions at electrolyte/film interface.

Chronocoulometry

Chronocoulometry (CC) gives quantitative information about the number of protons/ions intercalated or deintercalated on the application of a potential double step during a known amount of time [43]. The reversibility is then given by the ratio of the amount of charges deintercalated to the charges intercalated, i.e., $Q_{di}/Q_{i.}$. Figure 9 shows the CC plot of the NiO, Ni/PVP, NiO/PEG, and NiO/SDS thin films at a potential step of +1.4 to −1 V versus SCE in colored and bleached states for 10 s. The reversibility of all the samples were determined and listed in Table 1. The reversibility of NiO/SDS thin film was estimated to be 97%. As expected from the results of the contact angle and SEM images, the hydrophilic nature and a well-compact, smooth surface with nanoporous structure of the NiO/PVP, NiO/PEG, and NiO/SDS thin films show marginal enhancement in ion intercalation and deintercalation processes.

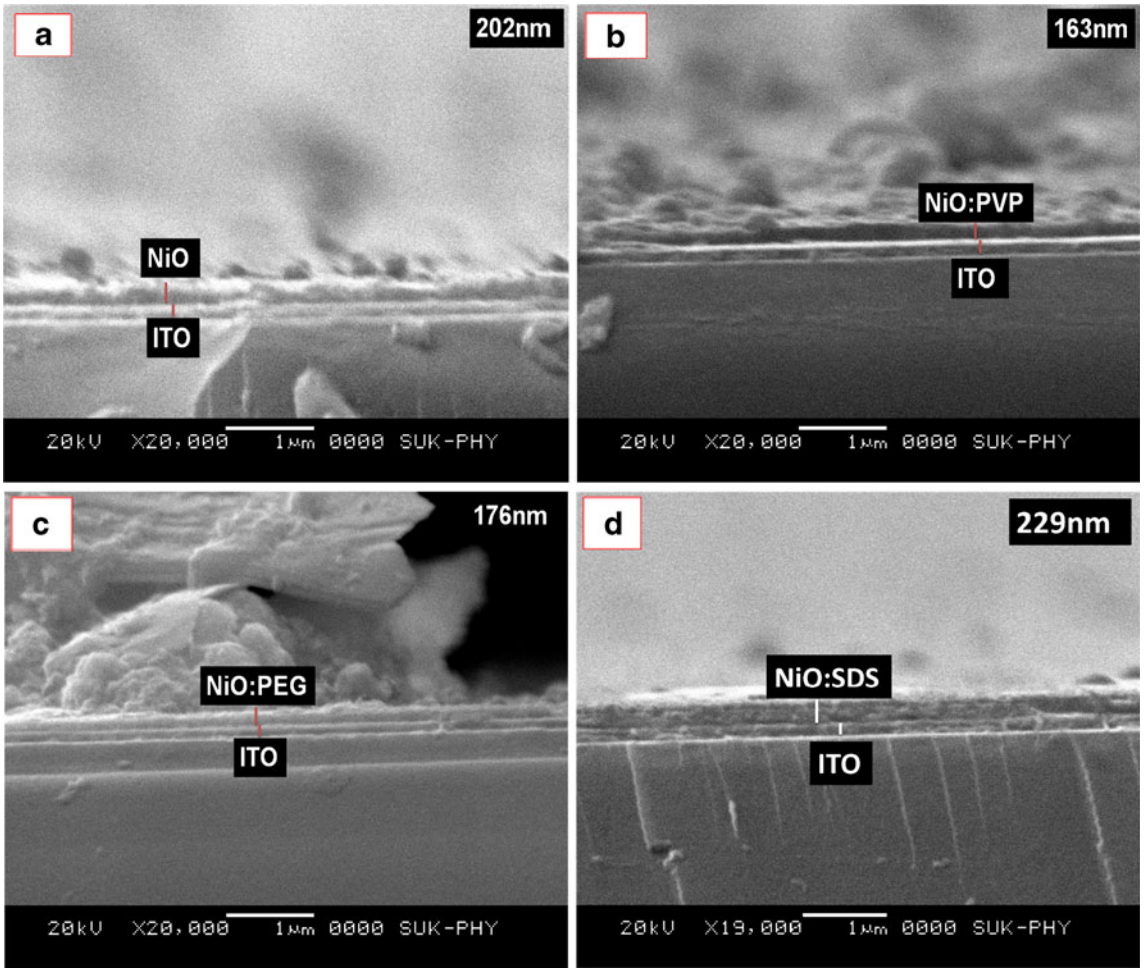

Fig. 4 Cross-section images of **a** NiO, **b** NiO/PVP, **c** NiO/PEG, and **d** NiO/SDS thin films

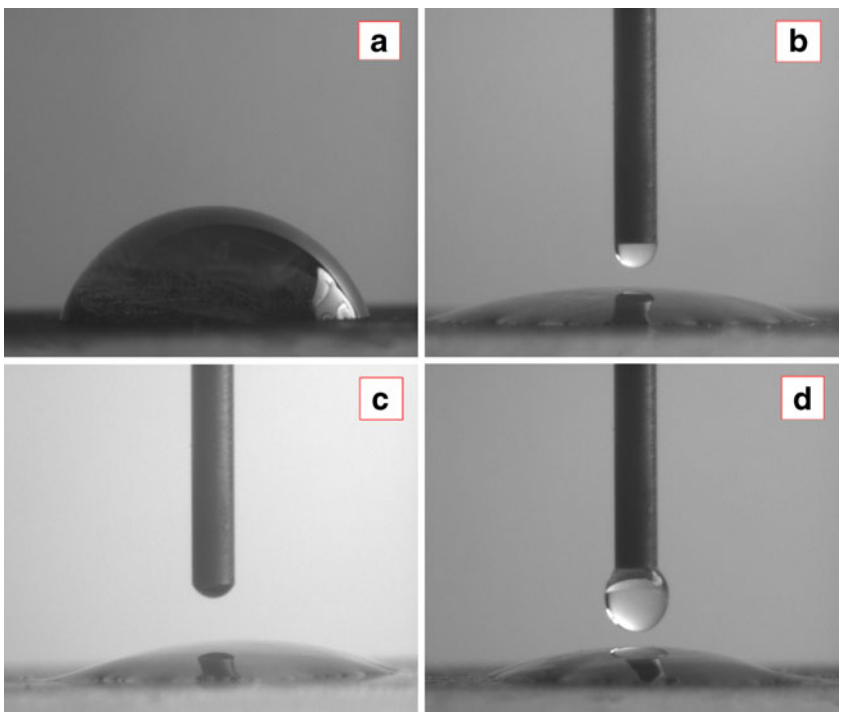

Fig. 5 Optical images of water droplets placed on **a** NiO, **b** NiO/PVP, **c** NiO/PEG and **d** NiO/SDS thin films

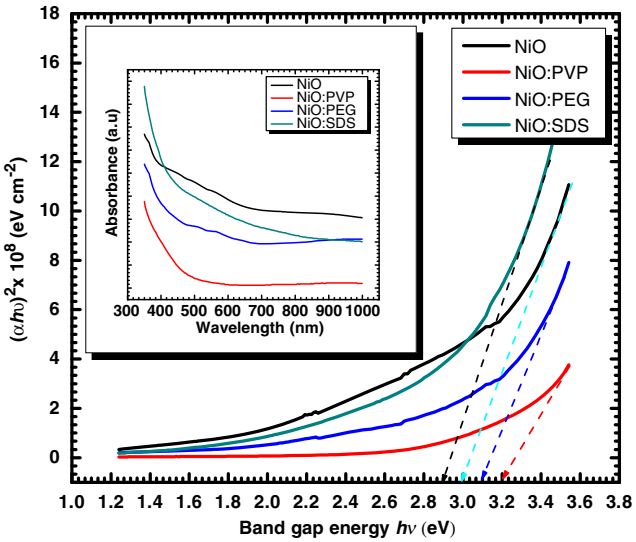

Fig. 6 Plots of $(\alpha h\nu)^2$ as a function of photon energy $(h\nu)$ for **a** NiO, **b** NiO/PVP, **c** NiO/PEG, and **d** NiO/SDS thin films annealed at 300 °C for 90 min. *Inset* shows the absorbance of NiO, NiO/PVP, NiO/PEG, NiO/SDS vs wavelength

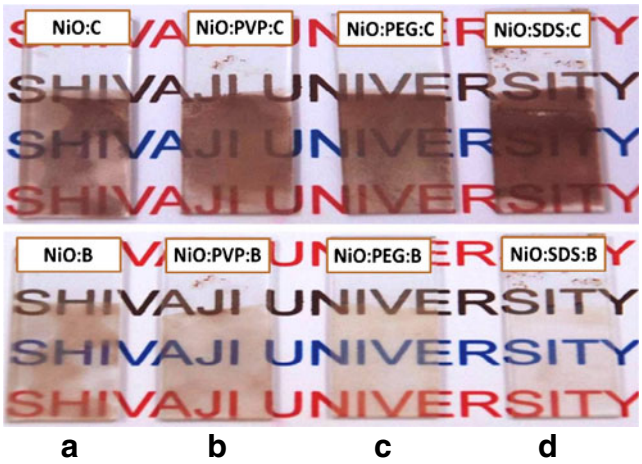

Fig. 8 Digital photograph of **a** pure NiO, **b** NiO/PVP, **c** NiO/PEG, and **d** NiO/SDS in their colored and bleached state (*C**=color, *B**=bleach)

Optical transmittance modulations and coloration efficiency

The optical transmission spectra for NiO, NiO/PEG, NiO/PVP, and NiO/SDS thin films in its colored and bleached states are shown in Fig. 10a–d. The optical transmittance difference (ΔT) in the colored and bleached states at 630 nm are found to be 31%, 32%, 38%, and 58%, for NiO, NiO/PVP, NiO/PEG, and NiO/SDS, respectively. The highest ΔT (57%) was observed for NiO/SDS thin film. The optical density difference and coloration efficiency (CE) of all the samples at 630 nm were calculated using relation Eqs. 5 and 6 and listed in Table 1.

$$\Delta OD = \ln\left(\frac{T_b}{T_c}\right)_{\lambda=630nm} \tag{5}$$

$$CE = \left(\frac{\Delta OD}{Q_i}\right)_{\lambda=630nm} \tag{6}$$

where T_b and T_c are the transmittance of the films in the bleached and colored state at λ=630 nm. CE is the

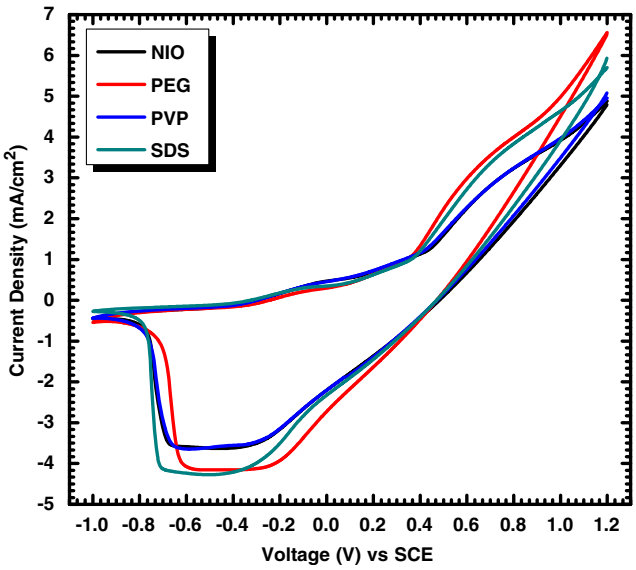

Fig. 7 Cyclic voltammogram of **a** pure NiO, **b** NiO/PVP, **c** NiO/PEG, and **d** NiO/SDS, recorded in 1 M KOH electrolyte. The potential was swept from −1 to +1.4 V vs SCE at a scan rate of 50 mV s^{-1}

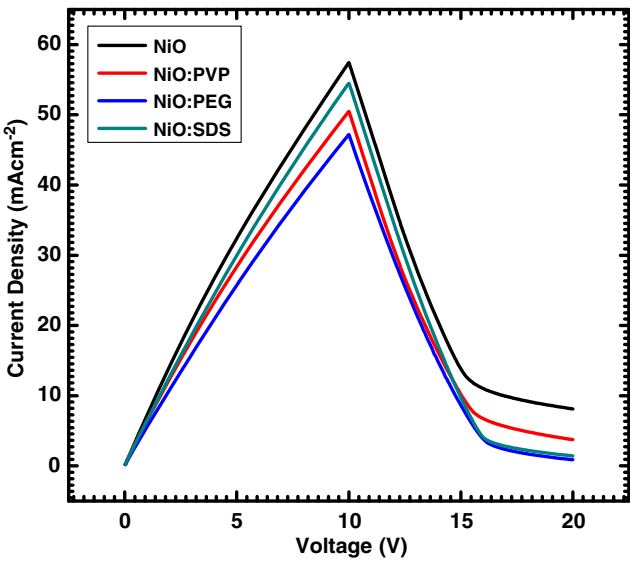

Fig. 9 Chronocoulometry curves of **a** pure NiO, **b** NiO/PVP, **c** NiO/PEG, and **d** NiO/SDS thin films recorded in 1 M KOH electrolyte upon application of step potential of −1 to +1.4 V vs SCE for 10 s after five cycles

Table 1 Parameters obtained from chronocoulometry and optical studies

Name	Thickness (nm)	Reversibility (%)	Transmittance (*T*b) (%) at 630 nm	Transmittance (*T*c) (%) at 630 nm	ΔT (%)	Optical density (ΔOD)	Coloration efficiency ($cm^2\ C^{-1}$)
NiO	202	85	69	38	31	0.58	25
NiO/PVP	163	92	59	27	32	0.78	39
NiO/PEG	176	98	66	28	38	0.85	44
NiO/SDS	229	97	83	25	58	1.16	54

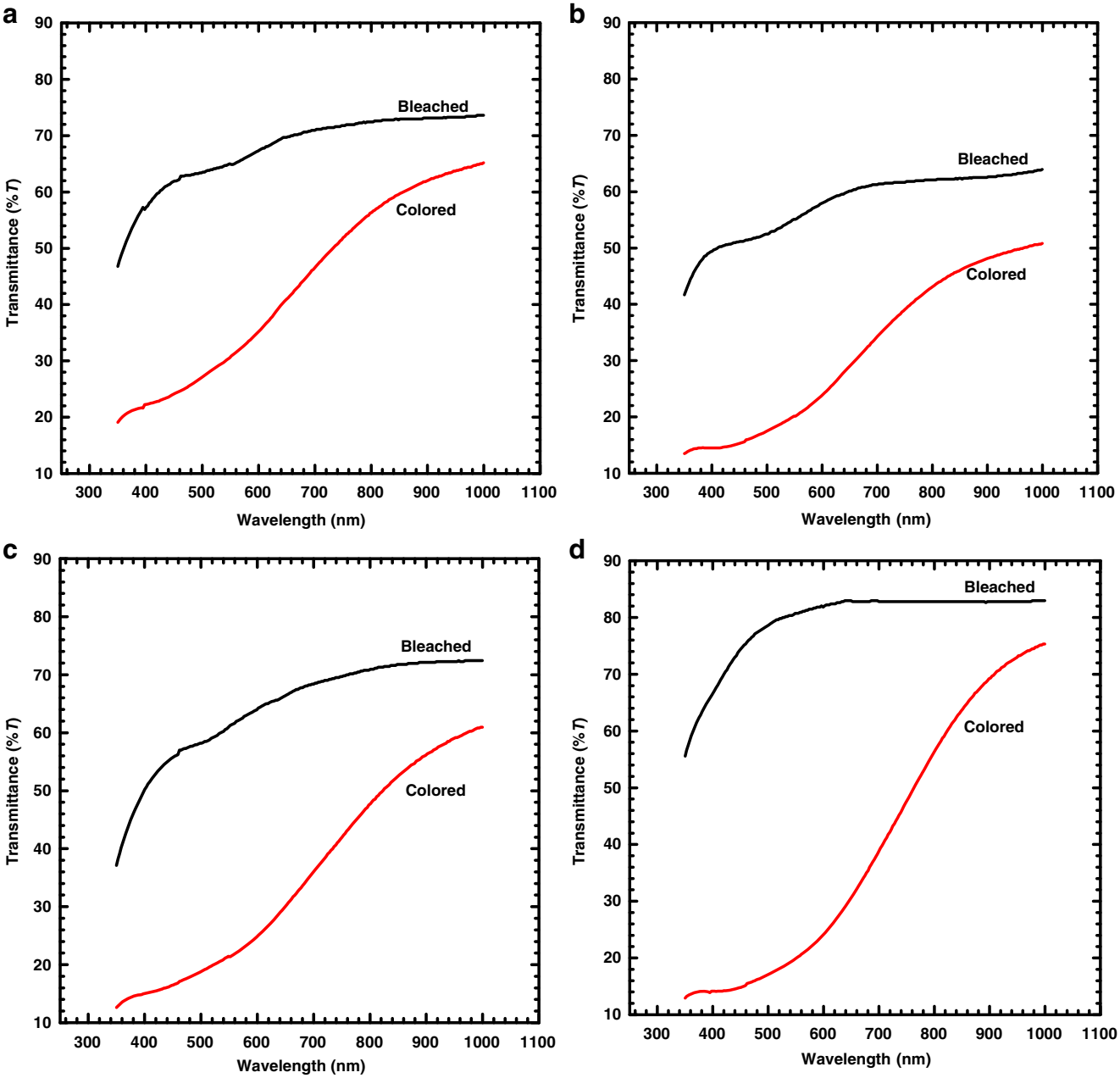

Fig. 10 Optical transmission spectra of **a** NiO, **b** NiO/PVP, **c** NiO/PEG, and **d** NiO/SDS thin films in their colored and bleached states after electrochemical polarization at −1 and +1.4 V vs SCE, recorded in the wavelength range of 350–1,000 nm

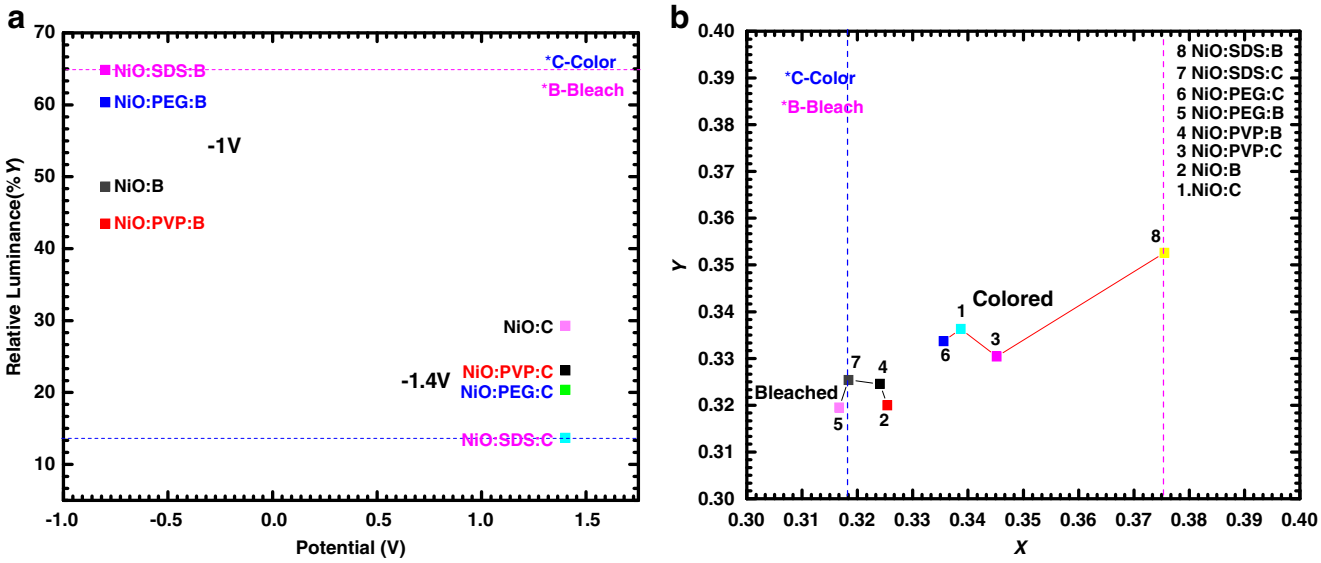

Fig. 11 **a** Relative luminance vs applied potential, for NiO, NiO/PVP, NiO/PEG, and NiO/SDS in their color/bleach state, the potential of −1 V was applied for bleaching and +1.4 V for coloring; (*dashed horizontal lines* indicate difference of relative luminance in their colored and bleached state for NiO/SDS), **b** CIE 1931 chromaticity diagram showing the (*x,y*) color coordinates for NiO, NiO/PVP, NiO/PEG, and NiO/SDS in their color/bleach state.(*dashed vertical lines* indicate difference of (*x,y*) in their colored and bleached state for NiO/SDS)

relation between ΔOD and Q_i and is approximately proportional to each other. The increase in ΔOD from pure NiO to NiO/SDS thin film leads to an increase in CE of about 54 cm^2 C^{-1} for NiO/SDS, which is higher than the reported [23, 28].

Colorimetric analyses

The colors of electrochemically deposited NiO, NiO/PEG, NiO/PVP, and NiO/SDS thin films were determined by performing colorimetric measurements [44] and were used

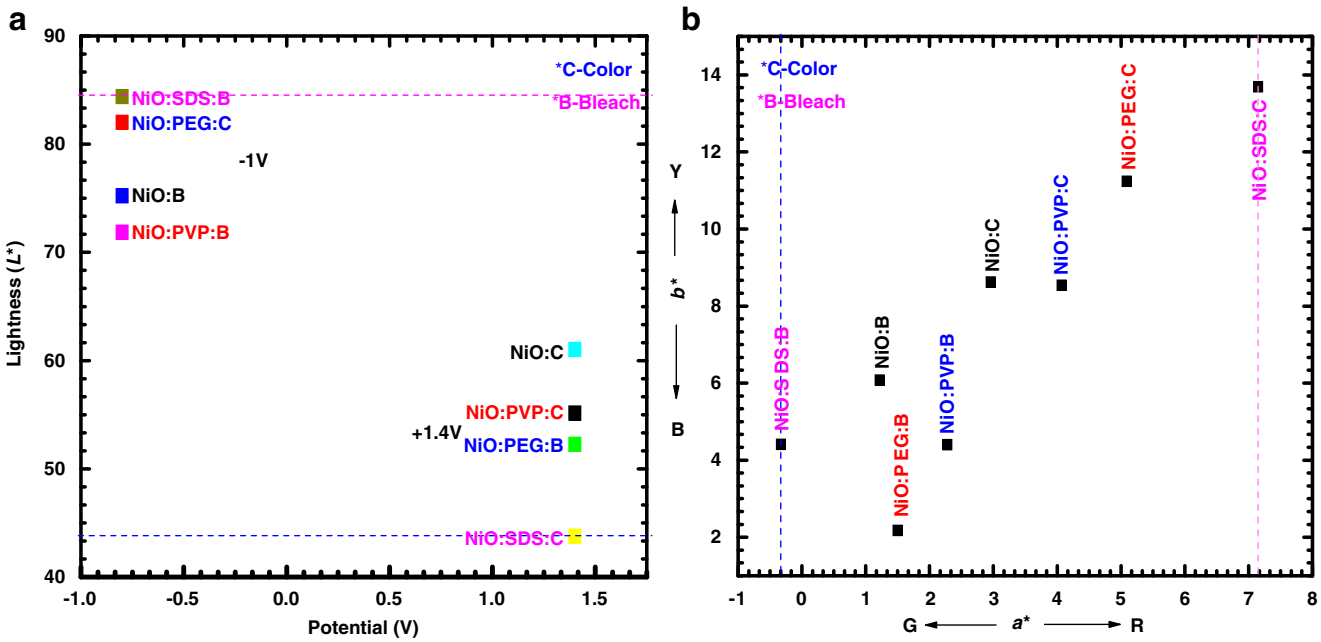

Fig. 12 CIE *L*a*b** coordinates of color **a** lightness of NiO, NiO/PVP, NiO/PEG, and NiO/SDS thin films in their color and bleach state upon application of potential step of −1 and +1.4 V, (*dashed horizontal lines* indicate difference of lightness in their colored and bleached state for NiO/SDS) **b** (*a*,b**) showing the hue and saturation for NiO, NiO/PVP, and NiO/PEG, NiO/SDS in their colored and bleached state upon application of potential step of −1 and +1.4 V (*dashed vertical lines* indicate difference of hue and saturation in their colored and bleached state for NiO/SDS). *L**=0 *dark*, 100 *white*, *a**= *red*(+)/*green*(−), and *b**=*yellow*(+)/*blue*(−)

as the quantitative scale to define the colors. The attributes of color, hue-*a* (its position between red and green, where negative value tends toward green and positive value tends toward red), saturation-*b* (its position in between blue and yellow, where negative value tends toward blue and positive value tends toward yellow) and lightness-*L* (where 0 is black and 100 is white) [45], were determined by analyzing the transmittance spectra of colored and bleach states after electrochemical polarization at +1.4 V (oxidized) and −1 V (reduced) state, respectively. In the CIE 1931 *Y*xy color space, the tristimulus value *Y* is defined as a measure of the brightness or luminance of the color [46] as shown in Fig. 11a. It shows the relative luminance (%*Y*) versus applied voltage for NiO, NiO/PEG, NiO/PVP, and NiO/SDS thin films in its colored and bleached state. It is observed that relative luminance (%*Y*) changes from 13% (colored) indicating deep brown to 65% (bleached) indicating colorlessness of NiO/SDS thin film, which is higher than that of NiO, NiO/PEG, and NiO/PVP. A two-dimensional *xy* representation, known as the chromaticity diagram (Fig. 11b) is utilized, in which *x* and *y* are calculated from the tristimulus values. As the potential is switched from −1 to 1.4 V vs SCE, a large change in the *xy* coordinates occurs as the color abruptly changes from highly transmissive (bleached) state to deep brown (colored) state for NiO/SDS thin film as compared with that of NiO, NiO/PEG, and NiO/PVP, as clearly evidenced from Fig. 8a–d. From CIE coordinates, lightness contrast was calculated to identify darkness/brightness corresponding to applied potential. Figure 12a shows the lightness of pure NiO, NiO/PEG, NiO/PVP, and NiO/SDS thin films in their colored and bleached state upon application of potential step of −1 to +1.4 V and corresponding lightness contrast were found to be 1.23, 1.30, 1.56, and 1.92. The highest lightness contrast (1.92) was observed for NiO/SDS thin film with corresponding color/bleach lightness difference of about 40.63%. On the basis of *xy* coordinates shown in Fig. 12b, anodic coloration (deep brown) and cathodic bleaching (colorlessness) of NiO/SDS is stronger as compared with that of NiO, NiO/PEG, and NiO/PVP. The color difference (ΔE^*) of NiO, NiO/PEG, NiO/PVP, and NiO/SDS thin films were calculated using the following relation [47].

$$\Delta E^* = \sqrt{\Delta L^2 + \Delta a^2 + \Delta b^2} \tag{7}$$

where ΔL, Δa, and Δb represent the difference between color/bleach states. The calculated color/bleach difference, ΔE^* for NiO/SDS thin film is found to be 42.69 which is higher than other samples.

Conclusions

Nanostructured NiO thin films with different morphologies were deposited by potentiostatic electrodeposition in the presence of various surfactants such as PVP, PEG, and SDS in nickel sulfate bath onto ITO-coated conducting glass substrate. The organic surfactants play a crucial role in tuning the surface morphological features, which is suitable for an intended application. SEM micrograph reveals that the well-compact, smooth surface with nanoporous structure made up of NiO/SDS thin film provides an easy path for electrolyte access into the film structure, which helps in improvement of EC performance. The wetting property of the NiO thin films with the aid of various surfactants is dictated by its surface structure, varying from slightly hydrophilic surface for pure NiO to superhydrophilic surface for NiO/SDS. The in situ colorimetric analysis method discussed in this paper is a significant step in the direction of precise measurement of the hue, saturation, and luminance of color states and allows the changes in these properties to be carefully monitored on redox (color/bleach) switching between electrochromic color states of pure and surfactants assisted NiO thin films. The ΔT of the NiO thin film in their colored and bleached state boosts by SDS additives with better electrochemical reversibility and coloration efficiency (97% and 54 cm^2 C^{-1}) due to formation of favorable microstructure coupled with superhydrophilicity.

Acknowledgment One of the authors, Mr. D. S. Dalavi, is thankful to University Grants Commission (UGC) for the award of Rajiv Gandhi Junior Research Fellowship and UGC-New Delhi for the financial support though UGC-New Delhi Project F.No.211/2008 (SR).

References

1. Granqvist CG (1995) Handbook of inorganic electrochromic materials. Elsevier, Amsterdam, pp 162–165
2. Yu PC, Nazri G, Lampert CM (1987) Sol Energy Mater 19:1
3. Hotovy I, Huran J, Spiess L, Hascik S, Rehacek V (1999) Sens Actuat B 57:147–152
4. Nattestad A, Ferguson M, Kerr R, Cheng Yi-B, Bach U (2008) Nanotechnology 19(295304):3852–3854
5. Ghosh M, Biswas K, Sundaresan A, Rao CNR (2006) J Mater Chem 16:106–111
6. Wei B, Yamamoto S, Ichikawa M, Li C, Takeshi F, Taniguchi Y (2007) Semicond Sci Technol 22:788–792
7. Sreethawong T, Suzuki Y, Yoshikawa S (2005) Int J Hydrogen Energy 30:1053–1062
8. Gomes A, da Silva Pereira MI (2006) Electrochim Acta 51:1342–1350
9. Kavinchan J, Thongtem T, Thongtem S (2010) Mater Lett 61:2388–2391

10. Zhu Z, Wei N, Liu H, Hea Z (2010) Advanced powder technology, In Press, Corrected Proof, Available online 1 July (doi:10.1016/j.apt.2010.06.008)
11. Cavalcante LS, Sczancoski JC, Tranquilin RL, Varela JA, Longo E, Orlandi MO (2009) Particuology 7:353–362
12. Thongtem T, Pilapong C, Kavinchan J, Phuruangrat A, Thongtem S (2010) J Alloy Comp 500:195–199
13. Phuruangrat A, Thongtem T, Thongtem S (2009) J Alloy Compd 481:568–572
14. Thongtem T, Jattukul S, Phuruangrat A, Thongtem S (2010) J Alloy Compd 491:654–665
15. Moura AP, Cavalcante LS, Sczancoski JC, Stroppa DG, Paris EC, Ramirez AJ, Varela JA, Longo E (2010) Adv Powder Technol 21:197–202
16. Inamdar AI, Mujawar SH, Ganesan V, Patil PS (2008) Nanotechnology 19:325706
17. Retter U, Tchachnikova M (2003) J Electroanal Chem 550:201–208
18. Opydo J (1992) Talanta 39:229–234
19. Lai WH, Shieh J, Teoh LG, Hung IM, Liao CS, Hon MH (2005) J Alloy Compd 396:295–301
20. Tan Y, Srinivasan S, Choi K-S (2005) J Am Chem Soc 127:3596–3604
21. Lee J, Hwang DK, Choi JM, Lee K, Kim JH, Im S (2005) Appl Phys Lett 87:023504
22. Nelson PA, Elliott JM, Attard GS, Owen JR (2002) J New Mater Electrochem Syst 5:63–65
23. Xia XH, Tu JP, Zhang J, Wang XL, Zhang WK, Huang H (2008) Electrochim Acta 53:5721–5724
24. Purushothaman KK, Muralidharan G (2008) J Sol Gel Sci Technol 46:90–94
25. Kamal H, Elmaghraby EK, Ali SA, Abdel-Hady K (2004) J Cryst Growth 262:424–434
26. Wang X, Song J, Gao L, Jin Ji, Zheng H, Zhang Z (2005) Nanotechnology 16:37
27. Uplane MM, Mujawar SH, Inamdar AI, Shinde PS, Sonavane AC, Patil PS (2007) Appl Surf Sci 251:9365–9371
28. Maruyama T, Arai S (1993) Sol Energy Mater Sol Cells 30:257–262
29. Penin N, Rougier A, Laffont L, Poizot P, Tarascon JM (2006) Sol Energy Mater Sol Cells 90:422–433
30. Nagai J (1993) Sol Energy Mater Sol Cells 31:291–299
31. Ahn KS, Nah YC, Sung YE (2003) Solid State Ionics 165:155–160
32. Avendan E, Azens A, Isidorsson J, Karmhag R, Niklasson GA, Granqvist CG (2003) Solid State Ionics 165:169–173
33. Wu MS, Yang CH (2007) Appl Phys Lett 91:033109
34. Huo QS, Margolese DI, Ciesla U, Demuth DG, Feng PY, Gier TE, Sieger P, Firouzi A, Chmelka BF, Schuth F, Stucky GD (1994) Chem Mater 6:1176–1181
35. Kadam LD, Patil PS (2001) Sol Energy Mater Sol Cells 69:361–369
36. Korosec RC, Ogorevc JS, Draskovic P, Drazic G, Bukovec P (2008) Thin Solid Films 516:8264–8271
37. Matar OK, Craster RV (2009) Soft Matter 5:801–808
38. Peng X, Chen A (2005) Appl Phys A 80:473–476
39. Dalavi DS, Suryavanshi MJ, Patil DS, Mali SS, Mohalkar AV, Kalagi SS, Vanalkar SA, Kang SR, Kim JH, Patil PS (2011) Appl Surf Sci. 257:2647–2656
40. Ezema FI, Ekwealor ABC, Osuji RU (2008) Superficies y Vacío 21(1):6–10
41. Sonavane AC, Inamdar AI, Shinde PS, Deshmukh HP, Patil RS, Patil PS (2010) J Alloy Compd 489:667–673
42. Lou X, Zhao X, Feng J, Zhou X (2009) Prog Org Coat 64:300–307
43. Kalagi SS, Dalavi DS, Pawar RC, Tarwal NL, Mali SS, Patil PS (2010) J Alloy Compd 493:335–339
44. CIE, Colorimetry (Official Recommendations of the International Commission on illumination) (1971) CIE Publication No15 Paris
45. Song HK, Lee EJ, Oh SM (2005) Chem Mater 17:2232–2233
46. Mortimer RJ, Reynolds JR (2005) J Mater Chem 15:2226–2233
47. Fei J, Lim KG, Palmore GTR (2008) Chem Mater 20(12):3832–3839